ARTICLE

ACS chemical biology

# Chromophore-Assisted Laser Inactivation of α- and γ-Tubulin SNAP-tag Fusion Proteins inside Living Cells

**Antje Keppler[†] and Jan Ellenberg[‡,*]**

[†]Virology, Hygiene Institute, University of Heidelberg, Im Neuenheimer Feld 324, Heidelberg D-69120, Germany and [‡]Cell Biology and Biophysics Unit, European Molecular Biology Laboratory (EMBL), Myerhofstrasse 1, Heidelberg D-69117, Germany

**ABSTRACT** Chromophore-assisted laser inactivation (CALI) can help to unravel localized activities of target proteins at defined times and locations within living cells. Covalent SNAP-tag labeling of fusion proteins with fluorophores such as fluorescein is a fast and highly specific tool to attach the photosensitizer to its target protein *in vivo* for selective inactivation of the fusion protein. Here, we demonstrate the effectiveness and specificity of SNAP-tag-based CALI by acute inactivation of α-tubulin and γ-tubulin SNAP-tag fusions during live imaging assays of cell division. Singlet oxygen is confirmed as the reactive oxygen species that leads to loss of fusion protein function. The major advantage of SNAP-tag CALI is the ease, reliability, and high flexibility in labeling: the genetically encoded protein tag can be covalently labeled with various dyes matching the experimental requirements. This makes SNAP-tag CALI a very useful tool for rapid inactivation of tagged proteins in living cells.

Chromophore-assisted laser inactivation (CALI) allows the functional analysis of a protein of interest inside live cells with high spatial and temporal resolution (*1*). At the same time it avoids disadvantages of other protein inactivation techniques, such as gene knockout or RNA interference, that suffer from genetic compensation and low time resolution as the effect of loss depends on the lifetime of the protein (*2*). For CALI and photodynamic therapy, photosensitizers are used that have a high quantum yield in reactive oxygen species (ROS) production upon intense light illumination at appropriate wavelengths. At low concentrations, ROS only oxidize proteins in their direct neighborhood, but at higher levels they are able to kill the cell (*3*).

Fluorescein has been the most widely used photosensitizer so far, and the relevant photochemical reactions that lead to protein inactivation have been analyzed in detail (*4*). Fluorescein has a high quantum yield for production of singlet oxygen that has been shown to be the reactive species damaging the target protein *via* photooxidation of methionine residues and cross-linking (*5*). Fluorescein proves to be 50 times more potent than malachite green, which was the first dye used for CALI (*6*). Singlet oxygen has a half-radius of photodamage of approximately 3−4 nm (*7*). As the average protein−protein interaction distance inside a cell is ~8 nm (*8*), the photosensitized protein is the primary target, but unspecific photodamage in the direct neighborhood always has to be controlled for in the case of fluorescein (*9*) as well as of other photosensitizers. Targeted to the protein of interest *via* specific, non-function-blocking antibodies, fluorescein has been used for high-throughput CALI set-ups (*10*). However, the technical difficulties as-

*Corresponding author, jan.ellenberg@embl.de.

Received for review October 8, 2008 and accepted January 9, 2009.

Published online February 3, 2009

10.1021/cb800298u CCC: $40.75

sociated with antibody-based CALI (injection of the antibody into the cell, specific binding to the target protein, risk of interference with the protein function upon antibody binding) have so far prevented a wide use of this in principle very attractive method. More robust techniques to target the photosensitizer dye to the protein of interest would therefore be very advantageous.

During the past decade new techniques were developed to add functionalities to proteins *in vitro* as well as *in vivo* that are not genetically encoded by the protein. The covalent and non-covalent binding of chemical compounds to peptide tags and fusion proteins opens manifold possibilities to characterize a protein of interest, influence its functionality, or simply purify it. Some prominent examples are the biarsenical-tetracysteine system, the Halo-Tag, and the β-galactosidase-, ACP-, CLIP-, or SNAP-tag labeling approaches (*11–17*). The most important parameters for all of these techniques are high labeling efficiency and specificity. The flexibility of labeling the same fusion construct with a variety of chemical compounds is a valuable advantage in comparison to purely genetically encoded tags such as fluorescent proteins. Once generated, the same fusion protein can be used for multiple types of experiments such as fluorescence microscopy applications, protein purification, or protein−protein interaction analysis, simply by varying the chemical compound that is bound to the tag.

A potential application of all of these techniques is the inactivation of the target protein labeled with a synthetic photosensitizer by CALI. The biarsenical-tetracysteine labeling system allows the specific binding of FlAsH-EDT2, a derivative of fluorescein, to a short peptide motif containing four cysteine residues that can be genetically fused to a protein of interest. When used for CALI, this approach was shown to inactivate synaptotagmin I and connexin-43 (*18, 19*). A second synthetic fluorophore binding to the tetracysteine motif is the so-called ReAsH (*19*). It has the advantage of an excitation maximum at a longer wavelength of 593 nm at which natural chromophores inside cells show less absorption than in the blue-light range. It is also a more potent photosensitizer than fluorescein, and the risk of unspecific photodamage is decreased due to lower illumination energies. However, this labeling technique was reported to show limitations in sensitivity and completeness of labeling, and the unspecific binding of biarsenical dyes to cysteines in endogenous proteins and the resulting high cytotoxicity have repeatedly been criticized (*20–22*) and require the addition of a competing dithiol reagent to decrease unspecific binding.

Lee *et al.* (*23*) recently reported a promising CALI approach based on the Halo-Tag labeled with Ru(II) tris(bipyridyl) dication, an efficient photocatalyst for singlet oxygen generation. However, more CALI experiments with specific inactivation in subcellular compartments need to be performed to evaluate the temporal and spatial resolution and specificity of this photosensitizer inside cells.

Furthermore, CALI has been developed based on genetically encoded photosensitizers that do not need any addition of external fluorophores, such as the autofluorescent proteins EGFP and Killerred (*24–26*). EGFP has been shown to inactivate α-actinin and focal adhesion kinase, but in comparison to fluorescein its CALI efficiency is much lower and in quantitative experiments it could only inactivate 40% of the target protein (*24*). The required light energies with EGFP are therefore in a range where unspecific photodamage to the cell can become an issue. To increase the efficiency of this approach, it has recently been combined with simultaneous knockdown of the unlabeled endogenous protein (*26*).

The dimeric protein Killerred shows its excitation maximum at 585 nm, combining the advantages of longer wavelength excitation and being a completely genetically encoded photosensitizer with a high quantum yield of singlet oxygen production (*25*). However like many multimeric fluorescent proteins, Killerred can induce the dimerization of its fusion partners, and therefore the use in CALI is limited until a monomeric variant is developed.

Here, we establish SNAP-tag labeling (originally described as labeling of AGT fusion proteins (*15*)) for CALI in living cells. The SNAP-tag consists of the human $O^6$-alkylguanine-DNA alkyltransferase (AGT), a 20-kDa protein that acts as a suicide enzyme to covalently transfer modifications from DNA bases onto itself. After it is fused to the target protein one desires to label, a synthetic probe is specifically attached to the SNAP-tag by irreversible transfer of the benzyl group from $O^6$-benzylguanine ($O^6$-BG) to a cysteine residue, resulting in a stable thioether bond (Figure 1) (*15, 27*). $O^6$-BG derivatives bearing a fluorescent dye at the *para*-position of the benzyl ring have been used for various imaging applications such as *in vivo* imaging of dynamic pro-

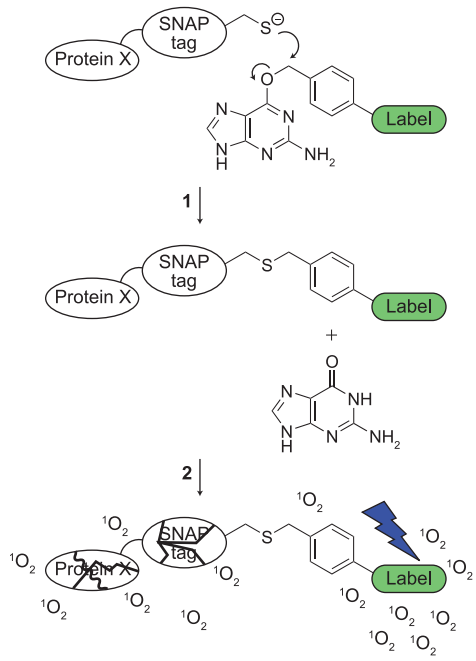


**Figure 1. SNAP-tag CALI based on the SNAP-tag labeling. Covalent labeling of SNAP-tag fusion proteins with $O^6$-benzylguanine derivatives bearing a fluorescent label (1). CALI of fluorophore-labeled SNAP-tag-protein X by illumination of the fluorophore with intense laser light at the appropriate wavelength (2). The production of singlet oxygen leads to the oxidation and therefore inactivation of the proteins in 3–4 nm proximity (*7*).**

cesses, fluorescence pulse chase experiments, and FRET applications (*15, 16, 28–30*). A major advantage of this approach is the availability of several cell-permeable fluorescent $O^6$-BG derivatives (*31*): BG diethylamino coumarin, BG diacetyl fluorescein (BGAF), BG Oregon Green, BG Rhodamine Green and TMRstar are available for direct intracellular live cell labeling, including the well-described photosensitizer fluorescein (*4*). Although they require microinjection, several longer wavelength dyes are also available (*30*).

We demonstrate the efficiency of SNAP-tag-based CALI by applying the technique to the inactivation of α- and γ-tubulin during mitosis. SNAP-tag-α-tubulin and γ-tubulin-SNAP-tag fusion proteins were labeled with the SNAP-tag substrate BGAF in mammalian cells and inactivated by illumination with an argon laser (488 nm) on a confocal microscope (Figure 1). The immediate effect on cell division is directly detected in live cells by confocal imaging. The inactivation of α-tubulin, one subunit of the heterodimer that makes up the lattice of microtubules (MTs), leads to dramatic changes in mitotic spindle morphology and arrest of the cell in metaphase. γ-Tubulin, another member of the tubulin family, is essentially involved in the nucleation of new MTs at microtubule-organizing centers (*32–34*). The inactivation of γ-tubulin reduced the number of nucleation events drastically and decreased the growth rates of MTs originating from the illuminated centrosome.

## RESULTS AND DISCUSSION

**CALI on SNAP-tag-α-tubulin in the Mitotic Spindle.** The metaphase spindle is a bipolar structure composed of highly dynamic MTs (*35, 36*). The astral MTs extend toward the cell cortex, the kinetochore MTs are attached with their plus end to the kinetochores of the chromosomes, and finally interpolar MTs overlap antiparallel in the midzone (Figure 4, panel a). The minus ends of all MTs direct toward the spindle poles. The dynamicity of the self-organizing spindle is essential to orchestrate chromosome segregation.

To establish SNAP-tag labeling as a tool for *in vivo* CALI, we set up a quantitative imaging assay in mitotic cells that allowed us to determine the illumination energy requirements and to detect the specific CALI effect in comparison to control experiments. For this purpose, we expressed SNAP-tag-α-tubulin in NRK cells and incubated the cells with the SNAP-tag substrate BGAF, a cell-permeable fluorescein derivative (*15*), resulting in specific labeling of the mitotic spindle (Figure 2, panel a). As photobleaching of fluorescein decreases its quantum yield for singlet oxygen production, cells targeted for CALI were not imaged with 488 nm excitation light before CALI illumination. Dividing cells in metaphase were selected by imaging the coexpressed chromosome marker H2B-mRFP (Figure 2, panel a) exclusively with a 594 nm HeNe laser line.

Instead of scanning the region of interest, the beam parc mode (irradiated beam area = 0.14 $\mu m^2$) provided by the Leica SP2 was used for CALI, thereby minimizing the phototoxic CALI illumination for the cell. Ten laser beam points were directed on one of the two spindle poles (Figure 2, panel b). Each point was illuminated for 250 ms and the total energy applied was 67.5 kJ $cm^{-2}$. After CALI, time lapse series of H2B-mRFP were acquired for each cell to monitor the CALI effect on mitotic progression of the cell. Upon CALI, the spindle stayed ar-

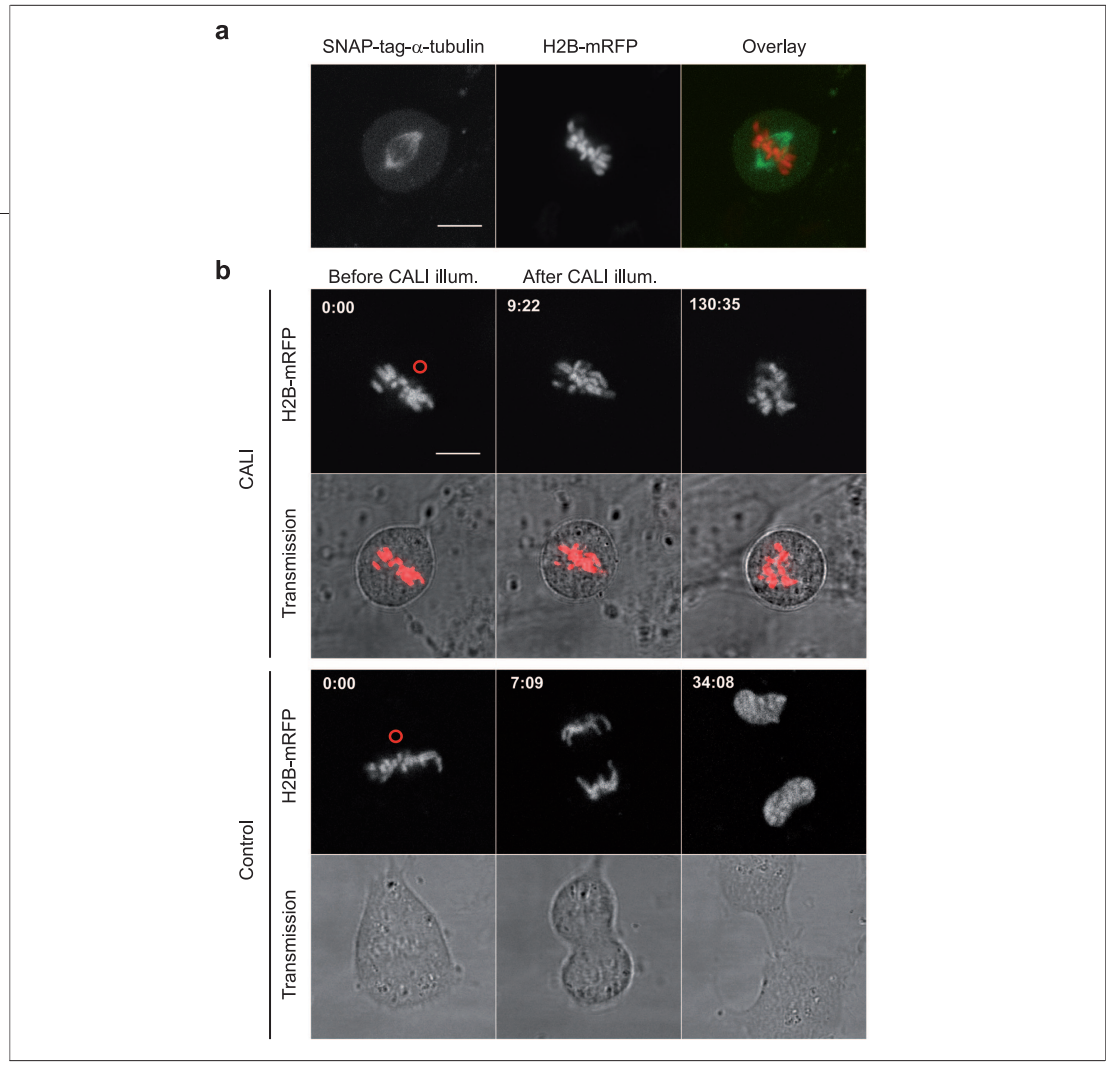


**Figure 2. CALI on fluorescein-labeled SNAP-tag-α-tubulin. a) NRK cell in metaphase expressing H2B-mRFP and SNAP-tag-α-tubulin labeled with BGAF (fluorescein). b) CALI on NRK cell (SNAP-tag-α-tubulin + BGAF, H2B-mRFP). Red ring defines the region of CALI illumination (67.5 kJ cm$^{-2}$) on the spindle pole. In the control sample, CALI illumination is performed as described except that this cell had not been incubated with BGAF for labeling SNAP-tag-α-tubulin. Time = min:sec. Size bar = 10 μm.**

rested in metaphase for 2 h (Figure 2, panel b). Afterwards, the chromosomes started to decondense and lost their metaphase plate alignment, and the cell arrested in the spherical shape it had adopted for mitosis.

To determine the minimal threshold energy required for this CALI effect on mitosis, we titrated the laser intensity and the duration of the laser beam (Supplementary Figure 1). For this experimental assay, we determined a threshold energy of 55 kJ cm$^{-2}$. Above this threshold, the CALI efficiency could not be further increased independent of the total illumination energy.

This threshold energy of the laser illumination is 100 times higher than for FlAsH CALI (*19*). This difference may account for the size of the tag, as SNAP-tag is a protein containing 182 amino acids in comparison to the tetracysteine-tag TC that comprises only 12 amino acids (*21*). The required amount of energy to produce a sufficient amount of ROS inactivating the target fusion protein will therefore be higher for SNAP-tag CALI because the SNAP-tag protein itself will first absorb ROS. However, SNAP-tag labeling has the advantage of being more rapid (<5 min) and highly efficient, specific and nontoxic covalent labeling, which makes SNAP-tag CALI much more suitable for live cell experiments. In general it is not possible to compare the values of total energy of the published CALI photosensitizers in a rigorous quantitative manner, as most of them use different target proteins, read-out assays, and technical set-ups.

For the SNAP-tag-α-tubulin we could achieve an arrest in metaphase for 78% ($n$ = 63) of the cells, when applying illumination energies above threshold (55 kJ cm$^{-2}$). This efficiency could not be increased by higher laser illumination, and 22% of all CALI-treated cells eventually proceeded into anaphase. However, analysis of the duration of metaphase in these cells revealed that there was a significant delay in progression when

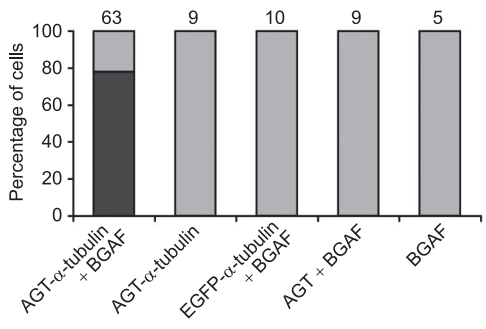


**Figure 3. Summarized results of CALI experiments on SNAP-tag-α-tubulin as described in Figure 2. Dark gray: arrest in metaphase; light gray: progress into anaphase. Seventy-eight percent of CALI-treated cells expressing SNAP-tag-α-tubulin labeled with BGAF were arrested in metaphase. Control samples: CALI illumination of unlabeled SNAP-tag-α-tubulin, EGFP-α-tubulin in the presence of BGAF, soluble SNAP-tag labeled with BGAF, and cells not expressing SNAP-tag-α-tubulin in the presence of BGAF.**

compared with control cells, also indicating that there was a CALI effect (unpublished data). This incomplete block in one-fifth of the cells could be due to a too-low amount of ROS production and thus SNAP-tag-α-tubulin inactivation.

**Specificity of CALI on SNAP-tag-α-tubulin.** In control samples, cells were not labeled with BGAF, but the experimental setup was otherwise identical to the CALI experiment. After illumination (67.5 kJ $cm^{-2}$), all control cells ($n = 9$) progressed into anaphase and divided into two daughter cells without any detectable abnormality (Figure 2, panel b and Figure 3). Thus, the intense laser illumination and the expression of SNAP-tag-α-tubulin do not effect mitotic progression. To demonstrate the specificity and the dependence of the close proximity of the fluorescein molecule to its target fusion protein, we CALI-treated cells expressing soluble SNAP-tag without a fusion partner and labeled it with BGAF and CALI-illuminated the cells ($n = 9$). All cells progressed normally through mitosis. Furthermore, cells ($n = 5$) not expressing any SNAP-tag fusion protein but incubated with BGAF always completed cell division normally after CALI illumination (Figure 3).

EGFP has been described as a CALI photosensitizer before (*24*). To compare the effectiveness of EGFP and SNAP-tag-fluorescein, we incubated NRK cells ($n = 10$) expressing EGFP-α-tubulin with BGAF and applied the highest CALI illumination energy (167.9 kJ $cm^{-2}$) available on our microscope system. In contrast to SNAP-tag-α-tubulin, all CALI-treated cells progressed into anaphase and no CALI-induced effect was detectable (Figure 3), demonstrating that SNAP-tag-fluorescein is more effective as a CALI photosensitizer than EGFP for α-tubulin under the given experimental conditions.

**CALI on Fluorescein-Coupled SNAP-tag-α-tubulin Causes Spindle Shortening.** To address by which mechanism CALI of fluorescein coupled SNAP-tag-α-tubulin causes metaphase arrest, we addressed the fate of the spindle after CALI illumination by correlative immunofluorescence using an α-tubulin antibody. Cells were CALI-illuminated and fixed at different time intervals after CALI to detect acute changes in spindle morphology (Figure 4, panel a). The spindle morphology of cells fixed 5 s after CALI illumination was indistinguishable from those in nontreated control cells. The spindle size and the density of MTs were comparable. However, cells that were fixed 4 min after CALI treatment had a shortened spindle, the number of MTs was reduced, and astral MTs were absent. After 12 min, the spindle had collapsed onto the chromosomes and reached a minimal size (Figure 4, panel a). Cells expressing EGFP-α-tubulin did not show any effect after identical CALI treatment, demonstrating again that fluorescein-labeled SNAP-tag is a considerably more sensitive CALI tool (Figure 4, panel a).

The effect on the spindle was always symmetrical, although the CALI illumination was only directed on one of the two spindle poles. Therefore we directed the laser beam for CALI illumination into the mitotic cytoplasm to see if the same spindle shortening is detected when soluble SNAP-tag-α-tubulin is inactivated. Indeed, the arrest in metaphase was observed also for cytoplasmic CALI-treated cells, and immunofluorescence analysis revealed the same decrease of the spindle size over time (data not shown). However, the total energy of the CALI illumination had to be almost twice as high (threshold = 96 kJ $cm^{-2}$, Supplementary Figure 1) to achieve the same efficiency as in the experiments with the laser beam directed onto the spindle pole (threshold = 55 kJ $cm^{-2}$, Supplementary Figure 1).

To determine how rapidly CALI inactivation of α-tubulin can affect the mitotic spindle, we measured the reduction of the spindle length using MAP4-mCherry as an *in vivo* marker for MTs. Immediately after CALI, cells were followed by time lapse imaging and the size

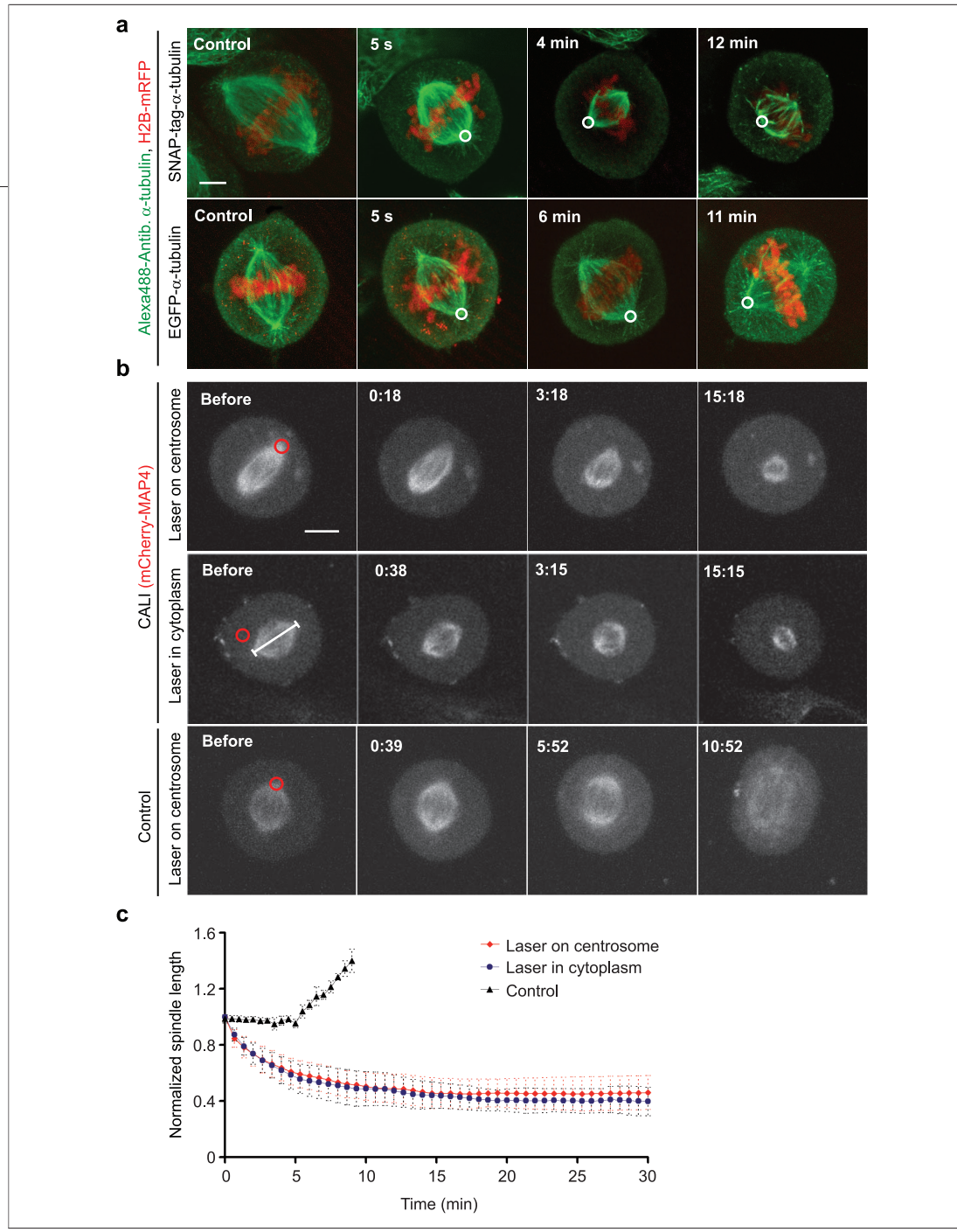


**Figure 4. Changes of spindle morphology after CALI on SNAP-tag-α-tubulin. a) Immunofluorescence analysis of CALI-treated cells (SNAP-tag-α-tubulin labeled with BGAF) with anti-α-tubulin antibody (Alexa488) at different time intervals after CALI illumination. Upper row: SNAP-tag-α-tubulin. Lower row: EGFP-α-tubulin. Controls were identical except for CALI illumination. Size bar = 5 μm. b) *In vivo* analysis of spindle size decrease by imaging MAP4-mCherry as a spindle marker. Upper row: the beam is directed at one spindle pole (67.5 kJ cm$^{-2}$). Middle row: the CALI laser beam is directed into the cytoplasm (96 kJ cm$^{-2}$). Lower row: control cells not labeled with BGAF, the beam is directed at one spindle pole (86 kJ cm$^{-2}$). c) For all CALI experiments the size of the spindle was determined for at least 6 different cells. Red = CALI on spindle. Blue = CALI in cytoplasm. Black - CALI on spindle pole in unlabeled control cells (normalized for anaphase onset). Time = min:sec. Size bar = 10 μm.**

of the spindle was determined at each time point (Figure 4, panel b). Cells were arrested in metaphase, and during the first 2 min after CALI, the spindle decreased already to about 50% of the final reduced spindle size that was reached after 15 min (0.51 ± 0.17 μm min$^{-1}$, $n$ = 7, Figure 4, panel c, red curve). Astral MTs and pole-to-pole MTs disappeared within minutes (Figure 4, panel a), and after prolonged arrest the

chromosomes lost their metaphase alignment, indicating that eventually also kinetochore fibers were affected. The dynamics of spindle size reduction were very similar, if CALI was performed with higher illumination energy (96 kJ $cm^{-2}$) on the soluble SNAP-tag-α-tubulin pool in the cytoplasm with a half-time of 2 and 19 min for the complete shortening process (0.50 ± 0.09 μm $min^{-1}$, $n = 6$, Figure 4, panel c, blue curve). The required energy for the same CALI effect when directing the laser beam into the cytoplasm was as seen before about 2-fold higher than for CALI on the centrosome, probably because of the higher local concentration of SNAP-tag-α-tubulin at the spindle pole in comparison to the cytoplasm. When using a subthreshold illumination energy of 51 kJ $cm^{-2}$ for CALI into the cytoplasm, cells progressed into anaphase with comparable kinetics as unlabeled control cells (Supplementary Figure 2).

The symmetric CALI effects first on dynamic and later on more stable spindle MTs were seen regardless whether the laser beam was directed on the centrosome or in the mitotic cytoplasm away from the spindle. A likely explanation is that SNAP-tag-α-tubulin oxidized by CALI interferes with new nucleation and polymerization of MTs. Since tubulin exchanges rapidly between the polymerized and unpolymerized state due to dynamic instability of spindle microtubule, this effect occurs both when SNAP-tag-α-tubulin is destroyed in the cytoplasm or in the spindle itself. A direct effect of oxidized SNAP-tag-α-tubulin damage while incorporated in polymerized MTs could not be detected, suggesting that the amount of SNAP-tag-α-tubulin incorporated into the microtubule lattice in addition to untagged endogenous tubulin was not sufficient to destabilize already polymerized MTs but required their turnover.

**Singlet Oxygen Is Responsible for the CALI Effect.** The molecular background of CALI based on fluorescein and the production of singlet oxygen as the reactive species have been studied thoroughly (*4*). Nevertheless, we wanted to confirm that SNAP-tag CALI on fluorescein-labeled fusion proteins is based on the same reaction mechanism. Therefore, we added the singlet oxygen quencher imidazole to cells or incubated them in oxygen-enriched medium during CALI, respectively. Applying the same CALI conditions as described in the previous experiments for SNAP-tag-α-tubulin, the addition of imidazole (final concentration = 15 mM) caused a reduction of the CALI efficiency by 36% ($n =$ 10). When adding imidazole to a final concentration of

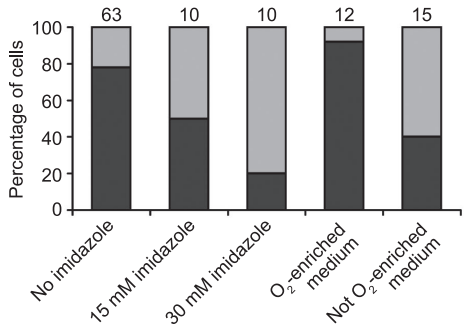


**Figure 5. Confirmation of singlet oxygen as reactive species of the CALI reaction. Imidazole (15/30 mM) is added to cells before CALI treatment (67.5 kJ $cm^{-2}$) to quench singlet oxygen. The CALI efficiency decreased by 36% and 74%, respectively. In contrast, CALI efficiency is increased 2.5-fold when cells are incubated in $O_2$-enriched medium in comparison to cells incubated in normal medium (here, CALI-treated with subthreshold CALI illumination energy of 23.5 kJ $cm^{-2}$).**

30 mM, the efficiency was decreased by 74% ($n = 10$) (Figure 5). When the cells were incubated in $O_2$-enriched medium, the efficiency was raised more than 2.5 fold ($n = 13$) in comparison to medium that had not been enriched with $O_2$ (applying subthreshold CALI illumination energy of 23.5 kJ $cm^{-2}$) (Figure 5). These experiments demonstrate the dependence of fluorescein-based SNAP-tag CALI on singlet oxygen as the reactive species.

**Inactivation of γ-Tubulin-SNAP-tag Demonstrates the Spatial Resolution of CALI.** To demonstrate that SNAP-tag-based CALI in a defined subcellular region can cause locally restricted specific protein damage, we performed CALI on centrosomal γ-tubulin-SNAP-tag. γ-Tubulin forms, in association with the γ-tubulin complex proteins, the γ-tubulin ring complex (γ-TuRC) that serves as seed for MT nucleation. The exact mechanism of nucleation of MTs at the γ-TuRC is still under investigation (*37*). The γ-TuRCs are found in soluble form in the cytoplasm as well as embedded into the pericentriolar material of the centrosome in a dynamic equilibrium. Khodjakov and Rieder (*38*) determined by FRAP experiments that the exchange of the dynamic pool of γ-tubulin at the centrosome takes about 60 min. A second pool of γ-tubulin has a longer residence time of about 5−6 h for a complete exchange. This fraction is thought to be bound to the centrioles. As our time series after CALI illumination comprises less than 2 min,

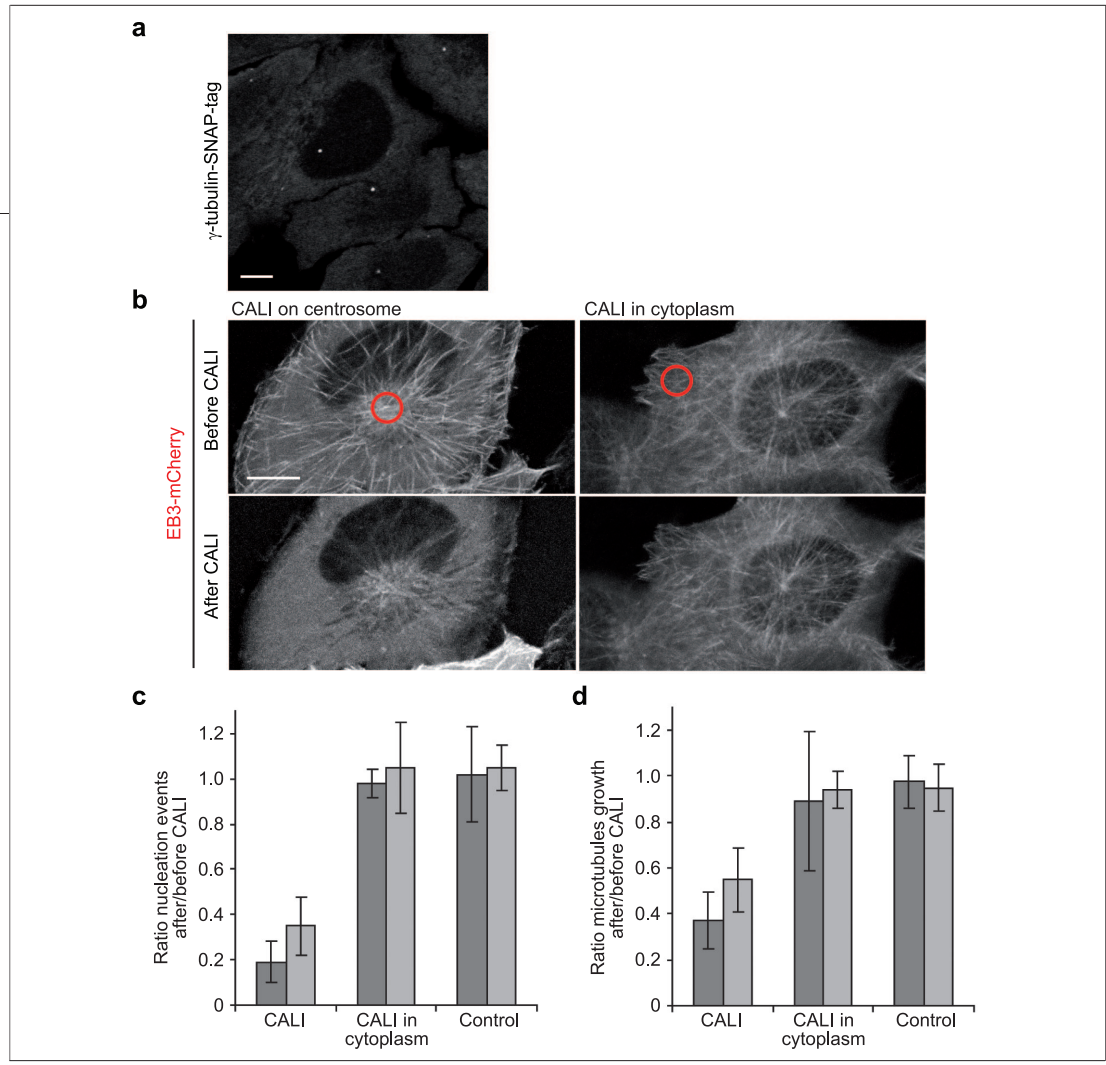


**Figure 6. CALI on γ-tubulin-SNAP-tag in cells coexpressing EB3-mCherry. a) HeLa cells stably expressing γ-tubulin-SNAP-tag labeled with BGAF. b) HeLa cell in late G2: EB3-mCherry highlights the plus end tips of growing MT emerging from the centrosome. Red circle indicates the region of applied CALI illumination on BGAF-labeled γ-tubulin-SNAP-tag. c) The ratio of nucleation events was determined for 10 individual cells before and after CALI illumination on the centrosome for CALI, in the cytoplasm or on centrosomes of unlabeled cells for control experiments. Dark gray = illumination with 10 laser beam points with 71 kJ $cm^{-2}$. Light gray = 4 laser beam points with 35.5 kJ $cm^{-2}$. d) For the same cells the change of MT growth rate after CALI illumination was determined by measuring kymographs on 10 single MTs per cell before and after CALI. Size bar = 10 μm. The error bars refer to the mean standard deviation for 10 individual cells.**

we expect that the exchange of CALI damaged versus cytoplasmic γ-tubulin-SNAP-tag has no significant influence on the result.

To interfere with the well-described function of γ-tubulin in MT nucleation, we established a HeLa Kyoto cell line stably expressing the fusion protein γ-tubulin-SNAP-tag (Figure 6, panel a). To directly image a potential effect on microtubule dynamics, EB3-mCherry, which binds to the plus end tips of growing MTs, was transiently expressed as a marker protein (*39, 40*). As before, we labeled the fusion protein γ-tubulin-SNAP-tag with BGAF, which resulted in specific centrosomal staining (Figure 6, panel a), and transferred the cells to a confocal microscope for CALI illumination and imaging. To prepare for mitosis, γ-tubulin accumulates at the maturating centrosome, and the MT nucleation capacity increases several fold to support the formation of the mitotic spindle (*38*). Therefore we chose cells in late G2 phase to interfere with γ-tubulin function *via* CALI. The centrosome position could be easily detected by the parallel accumulation of the marker protein EB3-mCherry, avoiding pre-illumination of the cells with the CALI wavelength. Before and 15 s after CALI illumination, time lapse series to document microtubule dynamics were recorded. For CALI, four laser beam points (71 kJ $cm^{-2}$) were directed on the centrosome.

Indeed, the number of nucleation events decreased by about 81% from 50.7 to 10.0 events $min^{-1}$ after CALI illumination of γ-tubulin-SNAP-tag in the centrosomal region (Figure 6, panel c). When using half the illumination energy (35.5 kJ $cm^{-2}$), the decrease was reduced to about 65%, confirming the dependence of CALI on the

total illumination energy (*41*). When the laser beam points were directed into the cytoplasm away from the centrosome, the number of nucleation events was not affected (Figure 6, panel c), demonstrating the spatial selectivity of this technique for protein inactivation. Cells expressing γ-tubulin-SNAP-tag that were not labeled with BGAF but CALI-illuminated under identical conditions did not show any reduction in the rate of nucleation (Figure 6, panel c).

Beside formation of new MTs in interphase, γ-tubulin plays an important role in mitotic spindle organization and, as was described recently, in the dynamics of MT plus ends (*42*). However, it is not understood how γ-tubulin contributes to the dynamic behavior of MT plus ends. In models for MT nucleation, γ-tubulin localization is restricted to the minus-end of MTs. It has been suggested that γ-tubulin complexes contribute to the loading of plus-end proteins onto new microtubule tips at the time of nucleation (*37*). This would be consistent with the detection of high concentrations of EB1 and other plus-end-binding proteins at the centrosome. Another possibility is that the localization of γ-tubulin complexes might not be restricted to the minus ends, and γ-tubulin could be present at low concentration along the MTs and at the plus-ends.

To address whether inactivation of γ-tubulin-SNAP-tag would not only decrease microtubule nucleation but also impair their growth (*42*), we determined the growth rate of individual MTs (Figure 6, panel d). To this end, we performed kymograph analysis of 10 MTs highlighted with EB3-mCherry, which emerged from the centrosome per cell. When comparing the values before and after CALI illumination, the growth rate decreased 64% from 18.54 (±3.20) to 6.66 (±1.68) μm $min^{-1}$ (71 kJ $cm^{-2}$, $n = 8$) and 45% from 18.29 ($cm^2$ 2.06) to 9.89 ($cm^2$ 2.21) μm $min^{-1}$ (35.5 kJ $cm^{-2}$, $n = 9$) after CALI (Figure 6, panel d). In control experiments, the same cells expressing γ-tubulin-SNAP-tag and EB3-mCherry were not labeled with BGAF but otherwise treated and CALI-illuminated under identical conditions. A difference in growth rate after CALI could not be detected (Figure 6, panel d). In a further control, cells were labeled with BGAF, but the laser beam points for CALI were directed in the cytoplasm, away from the centrosome. Again, no change in growth rate was seen. In summary, the specific inactivation of centrosomal γ-tubulin-SNAP-tag affected microtubule nucleation and growth rate and demonstrated the spatial selectivity of CALI based on fluorescein-labeled SNAP-tag fusion proteins.

The CALI treatment of γ-tubulin-SNAP-tag was effective in interfering with the described functions of this protein in MT nucleation and dynamics.

**Conclusion.** Here, we demonstrate the use of fluorescein-labeled SNAP-tag fusion proteins for CALI as a new tool for photoinactivation techniques to elucidate protein function inside living cells. The SNAP-tag CALI approach combines the advantages of a genetically encoded protein tag with the flexibility that synthetic fluorophores offer. The covalent and highly specific binding of the fluorophore allows the thorough removal of excess dye below measurable background, thereby diminishing the risk of unspecific photodamage. The *in vivo* labeling procedure is complete within 3−5 min, facilitating live cell experiments. The same SNAP-tag fusion construct can be labeled with various dyes with an increasing variety of properties concerning their photophysics, reactivities, or affinities to allow very different experimental set-ups for the same fusion protein. Here, we tested the SNAP-tag CALI approach with fluorescein as a photosensitizer, but this work opens the door for SNAP-tag based CALI applications using any photosensitizer conjugated to $O^6$-benzylguanine. In the future it will be desirable to develop additional cell permeable BG fluorophores, specifically, spectrally distinct photosensitizers. To further increase the efficiency of this CALI approach, the endogenous target protein can be knocked down by RNA interference, so that the tagged protein, if expressed in a stable and RNAi-resistant manner, is the only species in the cell that performs the biological function. We show that different SNAP-tag fusion proteins labeled *in vivo* with fluorescein can be inactivated in less than 1 s by laser illumination. The spatial resolution of this approach is restricted by the half-maximum range of the singlet oxygen. The illuminated volume for CALI inside the cell was as small as the confocal volume given by the optical parameters of the microscope settings (excitation wavelength 488 nm, numerical aperture 1.40, resolution in $xy = 0.2$ μm, resolution in $z = 0.8$ μm, confocal volume ≈ 1 fL). This allows addressing protein function inside cells with very high spatial and temporal resolution. Because it can be implemented readily on confocal laser scanning microscopes, inactivation of the protein can be combined with real time imaging of the dynamic cellular process under study as exemplified here by mitosis. SNAP-tag

based CALI could be used alone or in combination with complementing labeling techniques fitting the demand of the experimental setup. In combination with, *e.g.*, the tetracysteine-tag or the CLIP-tag, orthogonal CALI on different fusion proteins will be possible, addressing two or even more functions in one cell at the same time. As soon as additional cell-permeable photosensitizers with spectral properties different from those of BGAF are available, also sequential CALI solely based on the SNAP-tag will be possible.

So far, neither α-tubulin nor γ-tubulin have been targeted by CALI (*3*). As their functions are essential for fundamental and highly dynamic processes in the cell such as cell division and microtubule growth and nucleation, we hope that they will prove useful tools to elucidate their functional mechanism in the future.

## METHODS

The SNAP-tag approach was originally described as labeling of AGT fusion proteins and is now commercially available from Covalys Biosciences, who provided the BGAF used in this work.

**Constructs.** The construct SNAP-tag-α-tubulin has been described (*16*). The SNAP-tag mutant used in the γ-tubulin-SNAP-tag construct is identical to the mutant described in ref 16 except for two silent point mutations: residue His173 (CAC to CAT to remove the AgeI site) and residue Gln61 (CAG to CAA to remove the Apa LI site). The vector backbone of γ-tubulin-SNAP-tag is pEGFP-N1 (BD Biosciences, Palo Alto, CA), in which EGFP is replaced by SNAP-tag and γ-tubulin originating from construct γ-tubulin-mRFP (*43*) is inserted between the restriction sites *Bgl*II and *Eco*RI. pEB3-EGFP is a donation from N. Galjart (*44*). For EB3-mCherry, mCherry (a donation from R. Tsien (*45*)) was introduced between the restriction sites BsrGI and *Bam*HI in pEB3-EGFP, replacing EGFP. MAP4, a donation from J. B. Olmsted (*46*), was fused at its N-terminus to mCherry *via* the linker SKAAA to generate mCherry-MAP4, and the fusion protein was introduced between the restriction sites AgeI and *Eco*RI of pEGFP-C1 (BD Biosciences), replacing EGFP. H2B-mRFP has been published (*31*).

**Cell Culture.** A monoclonal stable HeLa Kyoto cell line expressing γ-tubulin-SNAP-tag was produced and maintained as described (*47*). The SNAP-tag-α-tubulin CALI experiments were performed on NRK cells transiently expressing SNAP-tag-α-tubulin. We did not notice a systematic correlation between CALI efficiency and expression level of SNAP-tagged α-tubulin. For live cell imaging, cells were cultured in Laboratory Tek II chambered coverglasses (No. 1; NalgeNunc International, Rochester, NY) and maintained at 37 °C in imaging medium [$CO_2$-independent Dulbecco's modified Eagle medium (DMEM; Invitrogen, Carlsbad, CA) without phenol red and supplemented with 20% fetal calf serum (FCS), 10 mM glutamine, penicillin/streptomycin] as described (*47*).

For the labeling with cell-permeable BGAF, cells were incubated with minimum essential medium (MEM) containing the labeling dye at a final concentration of 5 μM for 5 min. The cells were then washed three times with MEM before adding imaging medium. Imaging and CALI illumination was started 15 min after washing. Here, the minimal times for labeling and washing out of excess dye were 3 and 10 min, respectively.

**Imaging and CALI on Confocal Laser-Scanning Microscopes.** The CALI experiments were performed on a Leica SP2 AOBS Sirius (Leica Microsystems, Mannheim, Germany) confocal microscope. Cells were imaged and CALI-illuminated using the PL APO 63×/1.4-0.6 NA oil-immersion objective. For imaging H2B-mRFP and EB3-mCherry, a HeNe 2.5 mW, 594 nm laser was used at 20% and 90% transmission, respectively, and fluorescence emission was detected from 612 to 700 nm. To minimize the phototoxic effect of CALI and the unspecific damage inside the cell, CALI illumination was performed using the beam parc modus of the instrument and not the scanning mode. The focused laser beam was successively positioned at 10 different points stochastically distributed inside a region of interest, and each point was irradiated with the indicated dose and for the indicated time. The area of one beam point and therefore of a single irradiation was approximately 0.14 $\mu m^2$. If not mentioned otherwise, 10 beam points were directed at one of the two spindle poles (SNAP-tag-α-tubulin) in metaphase (identified in the transmitted light image) or the centrosomal region (γ-tubulin-SNAP-tag) in late G2 (identified by EB3-mCherry staining). The duration of excitation (typically 250 ms for each beam point) and the laser intensity (425 mW argon laser, 488 nm) were defined according to the experimental setup, and the resulting CALI illumination energies ranged from 23.5 to 167.9 kJ $cm^{-2}$ and are given in the results. The laser power was measured at the position of the specimen using the laser power meter Ophir Nova II (Ophir Optronics Ltd.). After CALI, live cell image sequences were acquired imaging H2B-mRFP to score mitotic progression or EB3-mCherry to score microtubule dynamics. For EB3-mCherry, 50 images per cell were recorded at 2 s intervals.

**Testing Singlet Oxygen As the Reactive Species of Fluorescein-Based SNAP-tag CALI.** For quenching CALI-produced singlet oxygen inside treated cells, imidazole was added to the cells to a final concentration of 15 or 30 mM, respectively, before CALI illumination. CALI experiments were performed as described above. For increase of singlet oxygen production upon CALI, we incubated the cells in freshly $O_2$-enriched medium before and during CALI. In this case, the applied CALI illumination energy was 23.5 kJ $cm^{-2}$ to detect an increase in CALI efficiency. In untreated medium the threshold was 55 kJ $cm^{-2}$ at which 78% of all CALI-treated cells were arrested in metaphase.

**Immunofluorescence on SNAP-tag-α-tubulin.** Cells were cultured in Laboratory Tek II chambered coverglasses and CALI-treated on the Leica SP2 system as described above. At different time points (see Figure 4) after CALI illumination cells were processed for immunofluorescence on the microscope to avoid loss of the loosely attached mitotic cells. Cells were fixed in a final concentration of 3% formaldehyde for 10 min. After the cells were washed three times carefully with PBS, an anti-α-tubulin antibody (diluted 1:1000, raised in mouse, T9026, Sigma-Aldrich) was added for 20 min, and an antimouse antibody conjugated with Alexa488 (diluted 1:1000, raised in goat, A11029, Molecular Probes) was added for detection. For comparison, non-CALI-treated control cells were imaged in the same Laboratory Tek to ensure identical immunofluorescence conditions.

**Image Processing.** The size of the spindle and the rate of microtubule nucleation were analyzed with the open source software ImageJ (http://rsb.info.nih.gov/ij/). For measuring the rate of microtubule nucleation, time lapse sequences were advanced frame by frame, and EB3-mCherry labeled microtubule tips emerging from the centrosome were counted interactively. Each

image sequence was evaluated three times. The variation of the repeated counts was less than 5%. Microtubule growth rates were determined with an in-house-developed kymograph macro (http://www.embl.de/eamnet/html/kymograph.html). Growth rates and tracks were analyzed with Excel (Microsoft). Figures were assembled with Illustrator and Photoshop (Adobe Systems).

*Acknowledgment:* We thank E. Dultz, S. Huet, M. Schuh, and L. Sironi for their support and critical reading of the manuscript. Werner Knebel from Leica Microsystems Mannheim is acknowledged for excellent collaboration to configure a confocal microscope for CALI. A.K. was supported by a FEBS long-term fellowship.

*Supporting Information Available:* This material is available free of charge *via* the Internet at http://pubs.acs.org.

## REFERENCES

1. Jay, D. G. (1988) Selective destruction of protein function by chromophore-assisted laser inactivation, *Proc. Natl. Acad. Sci. U.S.A. 85*, 5454–5458.
2. Dorsett, Y., and Tuschl, T. (2004) siRNAs: applications in functional genomics and potential as therapeutics, *Nat. Rev. Drug Discovery 3*, 318–329.
3. Hoffmann-Kim, D., Diefenbach, T. J., Eustace, B. K., and Jay, D. G. (2007) Chromophore-assisted laser inactivation, *Methods Cell Biol. 82*, 335–354.
4. Horstkotte, E., Schroder, T., Niewohner, J., Thiel, E., Jay, D. G., and Henning, S. W. (2005) Toward understanding the mechanism of chromophore-assisted laser inactivation—evidence for the primary photochemical steps, *Photochem. Photobiol. 81*, 358–366.
5. Yan, P., Xiong, Y., Chen, B., Negash, S., Squier, T. C., and Mayer, M. U. (2006) Fluorophore-assisted light inactivation of calmodulin involves singlet-oxygen mediated cross-linking and methionine oxidation, *Biochemistry 45*, 4736–4748.
6. Surrey, T., Elowitz, M. B., Wolf, P. E., Yang, F., Nedelec, F., Shokat, K., and Leibler, S. (1998) Chromophore-assisted light inactivation and self-organization of microtubules and motors, *Proc. Natl. Acad. Sci. U.S.A. 95*, 4293–4298.
7. Beck, S., Sakurai, T., Eustace, B. K., Beste, G., Schier, R., Rudert, F., and Jay, D. G. (2002) Fluorophore-assisted light inactivation: a high-throughput tool for direct target validation of proteins, *Proteomics 2*, 247–255.
8. Linden, K. G., Liao, J. C., and Jay, D. G. (1992) Spatial specificity of chromophore assisted laser inactivation of protein function, *Biophys. J. 62*, 956–962.
9. Guo, J., Chen, H., III, and Ikeda, S. R. (2006) Fluorophore-assisted light-inactivation produces both targeted and collateral effects on N-type calcium channel modulation in rat sympathetic neurons, *J. Physiol. 576*, 477–492.
10. Rubenwolf, S., Niewohner, J., Meyer, E., Petit-Frere, C., Rudert, F., Hoffmann, P. R., and Ilag, L. L. (2002) Functional proteomics using chromophore-assisted laser inactivation, *Proteomics 2*, 241–246.
11. Adams, S. R., Campbell, R. E., Gross, L. A., Martin, B. R., Walkup, G. K., Yao, Y., Llopis, J., and Tsien, R. Y. (2002) New biarsenical ligands and tetracysteine motifs for protein labeling *in vitro* and *in vivo*: synthesis and biological applications, *J. Am. Chem. Soc. 124*, 6063–6076.
12. Promega. ((2006)).
13. Komatsu, T., Kikuchi, K., Takakusa, H., Hanaoka, K., Ueno, T., Kamiya, M., Urano, Y., and Nagano, T. (2006) Design and synthesis of an enzyme activity-based labeling molecule with fluorescence spectral change, *J. Am. Chem. Soc. 128*, 15946–15947.
14. George, N., Pick, H., Vogel, H., Johnsson, N., and Johnsson, K. (2004) Specific labeling of cell surface proteins with chemically diverse compounds, *J. Am. Chem. Soc. 126*, 8896–8897.
15. Keppler, A., Gendreizig, S., Gronemeyer, T., Pick, H., Vogel, H., and Johnsson, K. (2003) A general method for the covalent labeling of fusion proteins with small molecules *in vivo*, *Nat. Biotechnol. 21*, 86–89.
16. Keppler, A., Pick, H., Arrivoli, C., Vogel, H. a., and Johnsson, K. (2004) Labeling of fusion proteins with synthetic fluorophores in live cells, *Proc. Natl. Acad. Sci. U.S.A. 101*, 9955–9959.
17. Gautier, A., Juillerat, A., Heinis, C., Jr., Kindermann, M., Beaufils, F., and Johnsson, K. (2008) An engineered protein tag for multiprotein labeling in living cells, *Chem. Biol. 15*, 128–136.
18. Marek, K. W., and Davis, G. W. (2002) Transgenically encoded protein photoinactivation (FlAsH-FALI): acute inactivation of synaptotagmin I, *Neuron 36*, 805–813.
19. Tour, O., Meijer, R. M., Zacharias, D. A., Adams, S. R., and Tsien, R. Y. (2003) Genetically targeted chromophore-assisted light inactivation, *Nat. Biotechnol. 21*, 1505–1508.
20. Hearps, A., Pryor, M., Kuusisto, H., Rawlinson, S., Piller, S., and Jans, D. (2007) The biarsenical dye Lumio™ exhibits a reduced ability to specifically detect tetracysteine-containing proteins within life cells, *J. Fluoresc. 17*, 593–597.
21. Martin, B. R., Giepmans, B. N., Adams, S. R., and Tsien, R. Y. (2005) Mammalian cell-based optimization of the biarsenical-binding tetracysteine motif for improved fluorescence and affinity, *Nat. Biotechnol. 23*, 1308–1314.
22. Stroffekova, K., Proenza, C., and Beam, K. G. (2001) The protein-labeling reagent FLASH-EDT2 binds not only to CCXXCC motifs but also non-specifically to endogenous cysteine-rich proteins, *Pflugers Arch. 442*, 859–866.
23. Lee, J., Peng, Y., Xiao, X., and Kodadek, T. (2008) A general system for evaluating the efficiency of chromophore-assisted light inactivation (CALI) of proteins reveals Ru(II) tris-bipyridyl as an unusually efficient "warhead", *Mol. BioSyst. 4*, 59–65.
24. Rajfur, Z., Roy, P., Otey, C., Romer, L., and Jacobson, K. (2002) Dissecting the link between stress fibres and focal adhesions by CALI with EGFP fusion proteins, *Nat. Cell Biol. 4*, 286–293.
25. Bulina, M. E., Chudakov, D. M., Britanova, O. V., Yanushevich, Y. G., Staroverov, D. B., Chepurnykh, T. V., Merzlyak, E. M., Shkrob, M. A., Lukyanov, S., and Lukyanov, K. A. (2006) A genetically encoded photosensitizer, *Nat. Biotechnol. 24*, 95–99.
26. Vitriol, E. A., Uetrecht, A. C., Shen, F., Jacobson, K., and Bear, J. E. (2007) Enhanced EGFP-chromophore-assisted laser inactivation using deficient cells rescued with functional EGFP-fusion proteins, *Proc. Natl. Acad. Sci. U.S.A. 104*, 6702–6707.
27. Pegg, A. E. (2000) Repair of O(6)-alkylguanine by alkyltransferases, *Mutat. Res. 462*, 83–100.
28. Gendreizig, S., Kindermann, M., and Johnsson, K. (2003) Induced protein dimerization *in vivo* through covalent labeling, *J. Am. Chem. Soc. 125*, 14970–14971.
29. Kindermann, M., George, N., Johnsson, N. a., and Johnsson, K. (2003) Covalent and selective immobilization of fusion proteins, *J. Am. Chem. Soc. 125*, 7810–7811.
30. Keppler, A., Kindermann, M., Gendreizig, S., Pick, H., Vogel, H., and Johnsson, K. (2004) Labeling of fusion proteins of O6-alkylguanine-DNA alkyltransferase with small molecules *in vivo* and *in vitro*, *Methods 32*, 437–444.
31. Keppler, A., Arrivoli, C., Sironi, L., and Ellenberg, J. (2006) Fluorophores for live cell imaging of AGT fusion proteins across the visible spectrum, *Biotechniques 41*, 167–170, 172, 174, 175.
32. Horio, T., Uzawa, S., Jung, M. K., Oakley, B. R., Tanaka, K., and Yanagida, M. (1991) The fission yeast gamma-tubulin is essential for mitosis and is organized at microtubule organizing centers, *J. Cell Sci. 99*, 693–700.
33. Stearns, T., and Kirschner, M. (1994) In vitro reconstitution of centrosome assembly and function: the role of γ-tubulin, *Cell 65*, 623–637.
34. Wiese, C., and Zheng, Y. (2006) Microtubule nucleation: γ-tubulin and beyond, *J. Cell Sci. 119*, 4143–4153.

35. Kline-Smith, S. L. a. W. C. E. (2004) Mitotic spindle assembly and chromosome segregation: refocusing on microtubule dynamis, *Mol. Cell 15*, 317–327.
36. Gadde, S., and Heald, R. (2004) Mechanisms and molecules of the mitotic spindle, *Curr. Biol. 14*, R797–R805.
37. Raynaud-Messina, B., and Merdes, A. (2007) γ-Tubulin complexes and microtubule organization, *Curr. Opin. Cell. Biol. 19*, 24–30.
38. Khodjakov, A., and Rieder, C. L. (1999) The sudden recruitment of γ-tubulin to the centrosome at the onset of mitosis and its dynamic exchange throughout the cell cycle do not require microtubules, *J. Cell Biol. 146*, 585–596.
39. Piehl, M., Tulu, S. U., Wadsworth, P., and Cassimeris, L. (2004) Centrosome maturation: measurement of microtubule nucleation throughout the cell cycle by using GFP-tagged EB1, *Proc. Natl. Assoc. Sci., U.S.A. 101*, 1584–1588.
40. Stepanova, T., Slemmer, J., Hoogenraad, C. C., Lansbergen, G., Dortland, B., De Zeeuw, C. I., Grosveld, F., van Cappellen, G., Akhmanova, A. a., and Galjart, N. (2003) Visualization of microtubule growth in cultured neurons *via* the use of EB3-GFP (end-binding protein 3-green fluorescent protein), *J. Neurosci. 23*, 2655–2664.
41. Liao, J. C., Roider, J., and Jay, D. G. (1994) Chromophore-assisted laser inactivation of proteins is mediated by the photogeneration of free radicals, *Proc. Natl. Acad. Sci. U.S.A. 91*, 2659–2663.
42. Paluh, J. L., Nogales, E., Oakley, B. R., McDonald, K., Pidoux, A. L., and Cande, W. Z. (2000) A mutation in gamma-tubulin alters microtubule dynamics and organization and is synthetically lethal with the kinesin-like protein pkl1p, *Mol. Biol. Cell 11*, 1225–1239.
43. Gerlich, D., Beaudouin, J., Gebhard, M., Ellenberg, J., and Eils, R. (2001) Four-dimensional imaging and quantitative reconstruction to analyse complex spatiotemporal processes in live cells, *Nat. Cell Biol. 3*, 852–855.
44. Patel, S. R., Richardson, J. L., Schulze, H., Kahle, E., Galjart, N., Drabek, K., Shivdasani, R. A., Hartwig, J. H., and Italiano, J. E., Jr. (2005) Differential roles of microtubule assembly and sliding in proplatelet formation by megakaryocytes, *Blood 106*, 4076–4085.
45. Shaner, N. C., Campbell, R. E., Steinbach, P. A., Giepmans, B. N., Palmer, A. E., and Tsien, R. Y. (2004) Improved monomeric red, orange and yellow fluorescent proteins derived from *Discosoma* sp. red fluorescent protein, *Nat. Biotechnol. 22*, 1567–1572.
46. Olson, K. R., and Olmsted, J. B. (1999) Analysis of microtubule organization and dynamics in living cells using green fluorescent protein-microtubule-associated protein 4 chimeras, *Methods Enzymol. 302*, 103–120.
47. Daigle, N., Beaudouin, J., Hartnell, L., Imreh, G., Hallberg, E., Lippincott-Schwartz, J., and Ellenberg, J. (2001) Nuclear pore complexes form immobile networks and have a very low turnover in live mammalian cells, *J. Cell Biol. 154*, 71–84.